Cooxidation of Ammonia and Ethanol in Supercritical Water, Part 1: Experimental Results

Jason M. Ploeger, Michael A. Mock, and Jefferson W. Tester
Department of Chemical Engineering, Massachusetts Institute of Technology, Cambridge, MA 02139

DOI 10.1002/aic.11127
Published online February 26, 2007 in Wiley InterScience (www.interscience.wiley.com).

The cooxidative effect of ethanol on ammonia oxidation in supercritical water was studied for a range of temperatures (655–705°C), initial ammonia (1–3 mM), ethanol (0–1.0 mM), and oxygen concentrations (0.7–5.0 mM), corresponding to fuel equivalence ratios ranging from 0.9 to 2.2 for the complete combustion of both organic species. With a stoichiometric amount of oxygen available for complete oxidation, the addition of ethanol on an equivalent molar basis was found to increase ammonia conversion from 20 to 65% at initial concentrations of 1 mM for each reactant, $T = 700°C$, $P = 246$ bar, and $\tau = 2.5$ s. Nitrous oxide was produced in much larger quantities for ammonia–ethanol cooxidation than for ammonia oxidation. Based on fractional yields of nitrogen product, this amounted to 40–75% for co-oxidation with ethanol versus 4–13% without ethanol present. © 2007 American Institute of Chemical Engineers
AIChE J, 53: 941–947, 2007
Keywords: supercritical water oxidation, ammonia, ethanol, co-oxidation, kinetics

Background and Motivation

Supercritical water is an excellent media for the destruction of organic compounds. Above the critical point of pure water ($T_c = 374°C$, $P_c = 221$ bar), organics and oxygen become soluble and can be reacted rapidly in a single phase in residence times of order 60 s or less. At typical operating conditions ($T = 450–650°C$, $P = 240–300$ bar), most H—C—N compounds are oxidized completely to water, carbon dioxide, and nitrogen. Heteroatoms in organic compounds such as chlorine, sulfur, and phosphorus are mineralized to their corresponding inorganic acids HCl, H_2SO_4, and H_3PO_4, which can be neutralized to provide salts and separated as a concentrated liquid brine or precipitated solid depending on mixture composition and temperature and pressure conditions. Supercritical water oxidation (SCWO) has most often been used to treat dilute organic waste streams that are difficult to remediate by other means. The SCWO process can effectively treat a wide range of toxic aqueous waste streams to acceptable destruction and removal efficiency (DRE) levels, which are often greater than 99.99%. Additional information on SCWO technology is available in the reviews by Modell,[1] Tester et al.,[2] Gloyna and Li,[3] Savage et al.,[4] Tester and Cline,[5] Savage,[6] Shaw and Dahmen,[7] and Kritzer and Dinjus.[8]

Model compounds studied in our laboratory include hydrogen,[9] carbon monoxide,[10] methane,[11] benzene,[12] methylphosphonic acid (MPA),[13] ethanol,[14] methyl *tert*-butyl ether (MTBE),[15] and ammonia.[16,17] Of these, ammonia is the most refractory molecule for SCWO, typically requiring temperatures above 600°C to observe measurable conversion at typical residence times of 60 s or less. Most nitrogen-containing waste streams, one of the most common being raw or partially treated sewage sludges, produce ammonia as an intermediate hydrolysate, which in turn must be oxidized to N_2. Ammonia oxidation in SCW can show heterogeneous catalysis effects with observed rates often dependent on the surface-to-volume (S/V) ratio and the composition of the reactor wall material. These catalytic effects have been described as a linear combination of a homogenous and heterogeneous oxidation mechanism.[16,18]

Ammonia cooxidation has been restricted to studies of product distribution at long residence times and high DRE levels corresponding to conversion greater than 99.99%.

Correspondence concerning this article should be addressed to J. W. Tester at testerel@mit.edu.

Hong et al.[19] reported roughly equal molar yields of nitrous oxide (N_2O) and nitrogen in the destruction of sewage, which consists of a complex mixture of refractory and labile compounds that includes ammonia and a wide variety of labile lignin-cellulosic and fatty acid hydrocarbons. In contrast, the work of Ploeger et al.[17] showed that the yield of nitrous oxide never exceeded 13% for the oxidation of pure ammonia. An attempt was made in our laboratory by Webley et al.[16] to cooxidize ammonia with methanol, but no increase in conversion was observed due to limitations on preheating and temperature measurement in the reactor. Cocero et al.[20] cooxidized ammonia, pyridine, acetonitrile, and aniline with isopropanol to near-complete destruction and measured trace (parts per million) nitrogen products (NOx, nitrates, and nitrites) in the effluent.

The goal of this study is to determine the effect of cooxidation with ethanol on ammonia SCWO kinetics. Ethanol was chosen as a cooxidant because its behavior has been characterized in the cooxidation of methylphosphonic acid and ethanol.[21] Insights gained from the methylphosphonic acid-ethanol system helped guide the study of the ammonia-ethanol system. The first of a two-part series, this paper reports the experimental ammonia conversion and product distribution data for ammonia-ethanol cooxidation. This data will be used in the second paper to guide the development of an elementary reaction rate mechanism for ammonia-ethanol cooxidation.

Experimental Apparatus

The plug flow reactor system used for the cooxidation experiments is essentially the same as used earlier by Sullivan[13] and in greater detail by DiNaro.[22] The reactor system is shown in Figure 1, and the key features are described below.

Oxidant and organic solutions were pressurized and fed into the reactor system by two independently controlled Rainin SD-200 HPLC pumps. The organic feed was prepared by dissolving ammonia (28–30%, VWR International) and ethanol (200 proof, Pharmco) in deionized water (18.2 MΩ cm). The oxidant feed was prepared by diluting concentrated hydrogen peroxide (H_2O_2, 28–30% in water, Aldrich Chemical Company) in deionized water. H_2O_2 has been experimentally verified to decompose to oxygen and water completely in the preheater section previously.[23] Both feed solutions were degassed with helium.

The organic and oxidant feedstreams were separately preheated in two stages before entering the reactor. The first stage employed direct ohmic heating (DOH), which heated the streams to reaction temperature using resistive heating by applying a voltage across 9.5-m lengths of 1/16 in. (1.6 mm) O.D. × 0.01 in. (0.25 mm) wall Hastelloy (HC-276) tubing. The temperature regulation of the DOH system was accomplished by controlling the applied voltage levels with two separate PID controllers (Omega, p/n CN9000A) using temperatures measured by two 1/32 in. (0.8 mm) Type K thermocouples located directly after the DOH preheater section. The last 0.5 m of the DOH preheater coils located outside of the insulated DOH housing were also traced with heat tape to minimize heat losses. The second stage maintained the temperature in the preheater tubing between the DOH system and the reactor inlet. In the 0.3-m section between the DOH thermocouples and the reactor sandbath, resistive cable heaters (Watlow, p/n 62H24A6X, 1/16 in. (1.6 mm) O.D. × 2 ft. (61 cm) long, 10 V, 240 W max.) were wrapped around the tubing to minimize heat losses. The power to the cable heaters was controlled by variable transformers. Upon entering the fluidized sandbath, each stream passed through an additional 5.2-m coiled length of 1/16 in. (1.6 mm) O.D. × 0.01 in. (0.25 mm) wall HC-276 tubing to ensure isothermality at

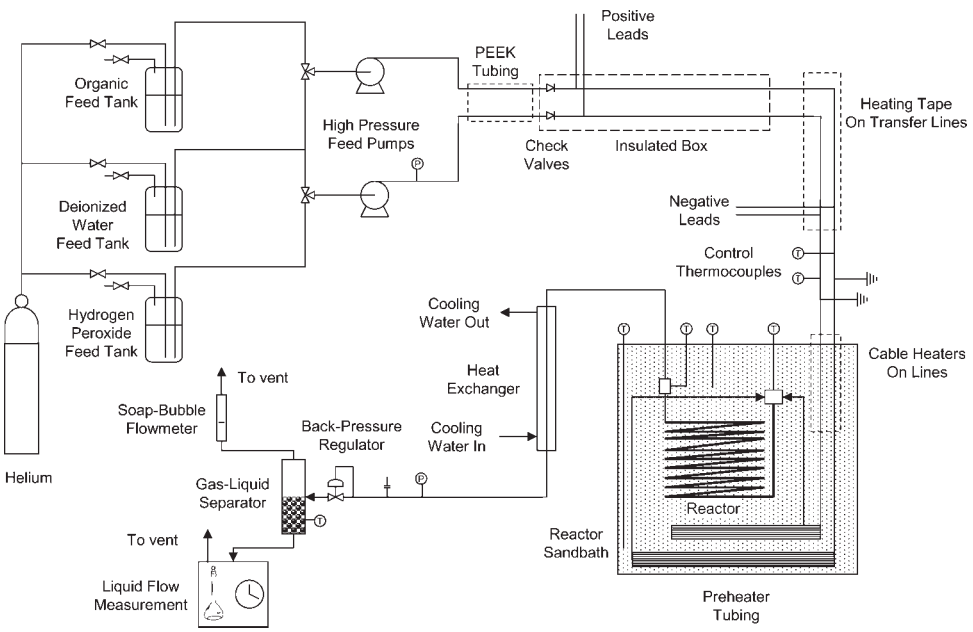

Figure 1. SCWO reactor system.

the reactor inlet to within the reproducibility of the thermocouples (±3°C).

The organic and oxidant streams were mixed in a modified 1/8 in. (3.2 mm) HC-276 cross from High Pressure Equipment (p/n 60-24HF2). The feedstreams entered the cross through two arms at an angle of 90° from each other. The internal diameters of the two arms were reduced from 1/16 in. (1.6 mm) I.D. to 0.01 in. (0.25 mm) I.D. by press fitting short lengths of 1/16 in. (1.6 mm) O.D. × 0.01 in. (0.25 mm) wall 316 SS (stainless steel) tubing into those arms. This modification was developed earlier by Phenix and Dinaro in our group to reduce the mixing time to values on the order of 0.5–1.0 s by increasing the velocities of the organic and oxidant feeds. Details of the design and evaluation of the mixing cross configuration are reported by Phenix et al.[23] A 1/16 in. Type K thermocouple was seated in a side port of the cross with its tip extended into the fluid to ensure accurate measurement of the fluid temperature. The fourth port of the cross was connected by an adapter (High Pressure Equipment, p/n 60-21HF4HF2) to the reactor inlet. The reactor was a 1/4 in. (6.36 mm) O.D. × 0.067 in. (1.7 mm) I.D. coiled length of Inconel 625 tubing with an internal volume of 10.71 ± 0.60 cm^3. A second 1/16 in. Type K thermocouple was seated in an 1/8 in. (3.2 mm) HC-276 tee (High Pressure Equipment, p/n 60-23HF2) at the reactor exit. A 26-cm length of 1/4 in. (6.36 mm) O.D. × 1/16 in. (1.6 mm) I.D. insulated HC-276 tubing rose out of the sandbath and connected to the heat exchanger. Temperatures measured by the four thermocouples mentioned previously and two 1/16 in. (1.6 mm) Type K thermocouples located in the top and bottom of the sandbath were monitored continuously with TracerDAQ software (Measurement Computing, p/n USB TC). The top and bottom sandbath temperature measurements were within the reproducibility of the thermocouples (±3°C).

After exiting the reactor, the effluent entered the inner tube of a shell-and-tube heat exchanger and was immediately quenched. The system pressure was controlled by a spring-loaded, manual backpressure regulator (Tescom, p/n 26-3200). Once the fluid exited the regulator, it flashed to atmospheric pressure and the resulting two-phase mixture was separated into two streams by the gas–liquid separator. The gas flow rate was measured using a soap bubble flowmeter and a stopwatch, and the liquid flow rate was measured by a 50-mL Class A volumetric flask and a stopwatch. Gas samples were withdrawn using a gas-tight syringe (Hamilton, p/n 1725) from the sampling port and were analyzed on gas chromatographs. Liquid samples were removed from the effluent and injected onto a gas chromatograph and an ion chromatograph.

For each experimental run, the reactor was stabilized for at least 1 h at each set of operating conditions to ensure steady-state operation. Measurements were then taken over the course of another hour or more where at least five liquid and gas samples were drawn and at least five liquid and gas flow rates were recorded to ensure reproducibility. The inlet ammonia and ethanol feed concentrations were measured from at least four samples, two taken at the beginning and at the end of the set of runs, to ensure that the feed concentrations remained constant. The H_2O_2 feed concentration was also sampled from the oxidant feed vessel at the beginning and at the end of the set of runs. The H_2O_2 feed concentration was measured by a ceric ion titration method to determine the oxygen concentration at the reactor inlet. The experimental precision for each measured concentration and flow rate was calculated to the 95% confidence level assuming a normal distribution.

All liquid samples were subjected to multiple analytical determinations of composition. An ammonium ion specific electrode (ThermoOrion p/n 9512) was used to measure the concentration of ammonia. An HP 6890 Series gas chromatograph (GC) employing a flame ionization detector (FID) with helium carrier gas was used to measure the concentration of ethanol, acetaldehyde, and methanol in all liquid samples. A 30 m × 0.53 mm I.D. × 1 μm film thickness DB-WAX column was used to separate the hydrocarbons.

To analyze the gas effluent, four separate gas chromatographs were used. For oxygen, nitrogen, carbon monoxide, and carbon dioxide, an HP 6890 GC was used with a thermal conductivity detector (TCD) using helium as the carrier gas. Two columns were connected in series with an air actuated switching valve. The first column was a 5 ft (1.5 m) × 1/8 in. (3.2 mm) 60–80 mesh Carboxen 1000 column, which separates the carbon-containing gases CO, CO_2, and CH_4 and connects to an 8 ft (2.4 m) × 1/8 in. (3.2 mm) 60/80 mesh Molsieve 5 Å column which separates the O_2 and N_2. An HP 5890 Series II GC with a TCD detector employed nitrogen as the carrier gas to analyze for helium and hydrogen. This GC also used the 60/80 mesh Carboxen 1000 and 60/80 mesh Molsieve 5 Å for separation. A second HP 5890 Series II GC with an FID detector used a helium carrier gas to analyze for light hydrocarbons, such as methane. The column was a bonded Astec PLOT column that can separate hydrocarbons up to C-10. To detect nitrogen oxides including nitrous oxide, nitric oxide, and nitrogen dioxide, a third HP 5890 Series II GC with an electron capture detector (ECD) and a DB-624 capillary column (J&W Scientific p/n 1153432) was used with helium carrier gas and nitrogen makeup gas.

Experimental Results

Experimental data were taken over a temperature range from 655 to 705°C at a pressure of 246 bar, initial ammonia concentrations ranging from 1 to 3 mM, and initial ethanol concentrations ranging from 0 to 1 mM. Temperatures cited are the average of the inlet and outlet temperatures. Introducing ethanol to the ammonia feed requires an addition of oxygen to maintain stoichiometric oxygen for both ammonia and ethanol. The fuel equivalence ratio is defined as

$$\Phi \equiv \frac{S_{NH_3}[NH_3]_o + S_{EtOH}[EtOH]_o}{[O_2]_o} \quad (1)$$

where S_i is the stoichiometric ratio of oxygen to fuel required for each compound ($S_{NH_3} = 0.75$ and $S_{EtOH} = 3$). Cooxidation experiments were conducted at stoichiometric oxygen ($\Phi = 1.00 \pm 0.05$) except for two fuel-rich experiments ($\Phi = 2.2 \pm 0.1$) and one pyrolysis/hydrolysis experiment with no added oxygen ($T = 700$°C, $P = 246$ bar, $[NH_3]_o = [EtOH]_o = 1$ mM, $[O_2]_o \approx 0$ mM, $\tau = 6.5$ s). The ammonia conversion in the pyrolysis experiment was (4 ± 2)%, which permits the assumption that ammonia does not significantly pyrolyze or hydrolyze in the preheaters.

Table 1. Summary of Experimental Data

Run No.	T (°C)	P (bar)	$[NH_3]_o$ (mM)	$[EtOH]_o$ (mM)	Φ	τ (s)	X_{NH_3} (%)	N balance (%)	N_2O yield (%)
1	701 ± 3	241 ± 1	1.03 ± 0.02	0.96 ± 0.04	0.95 ± 0.03	6.4 ± 0.4	75 ± 1	97 ± 3	29 ± 2
2	701 ± 3	245 ± 1	1.06 ± 0.03	0.99 ± 0.05	0.98 ± 0.04	4.5 ± 0.3	72 ± 1	90 ± 3	30 ± 2
3	698 ± 3	246 ± 1	1.08 ± 0.03	1.00 ± 0.05	0.99 ± 0.04	2.5 ± 0.2	64 ± 2	90 ± 2	38 ± 2
4	701 ± 3	241 ± 1	1.04 ± 0.02	0.97 ± 0.04	0.96 ± 0.03	5.4 ± 0.3	71 ± 1	92 ± 4	31 ± 2
5	699 ± 3	242 ± 1	1.05 ± 0.02	0.98 ± 0.04	0.98 ± 0.03	3.5 ± 0.2	70 ± 1	93 ± 2	42 ± 2
6	681 ± 3	242 ± 1	0.94 ± 0.03	0.97 ± 0.02	0.94 ± 0.03	6.4 ± 0.4	67 ± 1	100 ± 3	51 ± 3
7	680 ± 3	242 ± 1	0.94 ± 0.03	0.97 ± 0.02	0.95 ± 0.03	4.5 ± 0.3	66 ± 1	99 ± 3	55 ± 3
8	655 ± 3	244 ± 1	0.97 ± 0.02	0.97 ± 0.03	0.97 ± 0.03	6.6 ± 0.4	52 ± 1	109 ± 2	68 ± 2
9	652 ± 3	243 ± 1	0.98 ± 0.02	0.98 ± 0.03	0.97 ± 0.03	4.6 ± 0.3	49 ± 1	107 ± 2	71 ± 3
10	703 ± 3	241 ± 1	0.97 ± 0.02	0.95 ± 0.03	2.18 ± 0.09	6.4 ± 0.4	16 ± 2	97 ± 4	7 ± 2
11	701 ± 3	242 ± 1	0.96 ± 0.02	0.96 ± 0.04	2.18 ± 0.09	4.0 ± 0.2	15 ± 3	97 ± 3	14 ± 1
12	703 ± 3	242 ± 1	0.95 ± 0.03	0.09 ± 0.00	0.93 ± 0.04	6.4 ± 0.4	63 ± 2	109 ± 3	18 ± 1
13	703 ± 3	244 ± 1	0.96 ± 0.03	0.09 ± 0.00	0.93 ± 0.04	4.5 ± 0.3	54 ± 2	108 ± 3	20 ± 1
14	702 ± 3	243 ± 1	0.96 ± 0.02	0.09 ± 0.00	0.94 ± 0.03	3.4 ± 0.2	46 ± 2	107 ± 2	25 ± 1
15	705 ± 3	243 ± 1	3.00 ± 0.05	0.98 ± 0.02	1.05 ± 0.04	6.4 ± 0.4	72 ± 1	104 ± 2	34 ± 2
16	704 ± 3	244 ± 1	3.02 ± 0.05	0.99 ± 0.01	1.05 ± 0.04	4.5 ± 0.3	67 ± 1	103 ± 2	35 ± 2
17	704 ± 3	244 ± 1	3.01 ± 0.05	0.99 ± 0.02	1.04 ± 0.04	3.4 ± 0.2	62 ± 1	100 ± 2	33 ± 1
18	698 ± 4	243 ± 1	1.04 ± 0.03	0.48 ± 0.01	0.99 ± 0.04	6.4 ± 0.4	69 ± 2	112 ± 4	44 ± 2
19	694 ± 3	246 ± 1	1.06 ± 0.04	0.49 ± 0.02	0.99 ± 0.04	2.5 ± 0.2	53 ± 2	110 ± 3	58 ± 3
20	681 ± 3	243 ± 1	0.96 ± 0.02	1.00 ± 0.03	0.99 ± 0.04	4.5 ± 0.3	65 ± 1	113 ± 3	64 ± 4
21	677 ± 3	244 ± 1	0.97 ± 0.02	1.01 ± 0.03	1.00 ± 0.04	2.6 ± 0.2	58 ± 1	113 ± 4	73 ± 5
22	681 ± 3	241 ± 1	0.94 ± 0.03	0.00 ± 0.00	0.87 ± 0.03	6.6 ± 0.4	20 ± 3	104 ± 3	
23	681 ± 3	241 ± 2	0.94 ± 0.02	0.00 ± 0.00	0.87 ± 0.03	4.6 ± 0.3	17 ± 3	102 ± 3	
24	680 ± 3	242 ± 1	0.94 ± 0.02	0.00 ± 0.00	0.87 ± 0.03	3.1 ± 0.2	16 ± 2	97 ± 2	
25	680 ± 3	242 ± 1	0.96 ± 0.02	0.00 ± 0.00	0.95 ± 0.03	6.4 ± 0.4	21 ± 2	100 ± 2	4 ± 0
26	679 ± 3	242 ± 1	0.96 ± 0.02	0.00 ± 0.00	0.96 ± 0.03	4.5 ± 0.3	13 ± 2	102 ± 2	5 ± 0
27	677 ± 3	242 ± 1	0.97 ± 0.02	0.00 ± 0.00	0.97 ± 0.03	2.5 ± 0.1	11 ± 2	98 ± 2	4 ± 0
28	658 ± 3	244 ± 1	0.87 ± 0.02	0.00 ± 0.00	0.89 ± 0.04	6.5 ± 0.4	15 ± 3	101 ± 3	
29	656 ± 3	244 ± 1	0.87 ± 0.02	0.00 ± 0.00	0.88 ± 0.04	4.6 ± 0.3	13 ± 3	99 ± 3	
30	655 ± 3	244 ± 1	0.88 ± 0.02	0.00 ± 0.00	0.90 ± 0.04	2.5 ± 0.1	7 ± 3	100 ± 3	
31	698 ± 3	242 ± 1	0.94 ± 0.01	0.00 ± 0.00	0.92 ± 0.03	2.5 ± 0.1	20 ± 2	101 ± 2	5 ± 0
32	698 ± 3	244 ± 1	0.93 ± 0.02	0.00 ± 0.00	0.89 ± 0.03	4.5 ± 0.3	33 ± 2	102 ± 2	4 ± 0
33	702 ± 3	243 ± 1	0.93 ± 0.02	0.00 ± 0.00	0.96 ± 0.05	8.9 ± 0.5	58 ± 1	104 ± 3	4 ± 0
34	696 ± 3	243 ± 1	1.01 ± 0.03	0.00 ± 0.00	0.73 ± 0.03	6.5 ± 0.4	61 ± 2	104 ± 4	6 ± 0
35	697 ± 3	242 ± 1	1.01 ± 0.03	0.00 ± 0.00	0.73 ± 0.03	4.5 ± 0.3	42 ± 3	107 ± 4	7 ± 0
36	697 ± 3	243 ± 1	1.02 ± 0.02	0.00 ± 0.00	0.73 ± 0.02	3.5 ± 0.2	38 ± 2	104 ± 3	7 ± 0

Empty cells indicate data not available.
Φ = Fuel equivalence ratio (Eq. 1).
X_{NH_3} = Conversion of ammonia.
τ = Residence time, assuming plug flow conditions.

Experimental results are summarized in Table 1, with the precision errors for each experimental measurement reported at the 95% confidence interval. The only ammonia oxidation products observed were N_2 and N_2O. The nitrogen balance for ammonia–ethanol cooxidation runs closed within experimental error of (100 ± 10)%, which is a larger error than the pure ammonia oxidation data (100 ± 3%). The increased error is attributed to errors in measuring nitrous oxide in the reactor effluent, since N_2O yields were much higher in the cooxidation runs. The high solubility of N_2O in water multiplies the error in measuring N_2O in the gas phase because the molar flowrate of N_2O in the liquid effluent is calculated using a Henry's Law approximation, whereby it is assumed that the concentration in the liquid phase is linearly proportional to partial pressure in the gas phase.[24] No carbon products other than carbon dioxide were observed in the reactor effluent for cooxidation experiments, which supports the assumption that at such high temperatures ethanol oxidation would be rapid and complete.

The effect of initial ethanol concentration on ammonia conversion is shown in Figure 2. Increases in ammonia con-

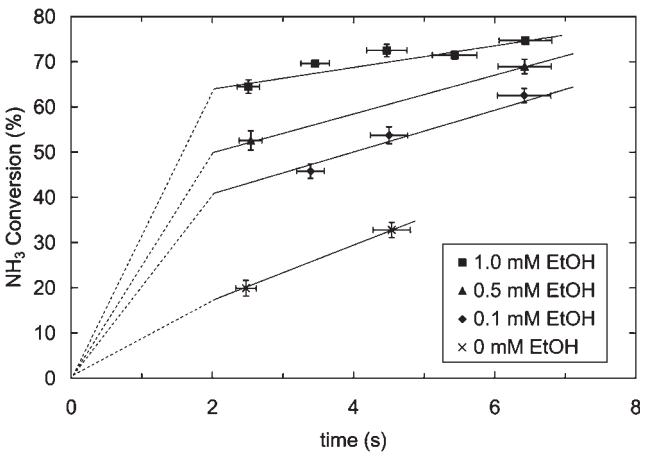

Figure 2. Ammonia conversion as a function of time for four different initial concentrations of ethanol.

T = (699 ± 5)°C, P = 243 ± 3 bar, $[NH_3]_o$ = 1.00 ± 0.08 mM, and Φ = 0.95 ± 0.05.

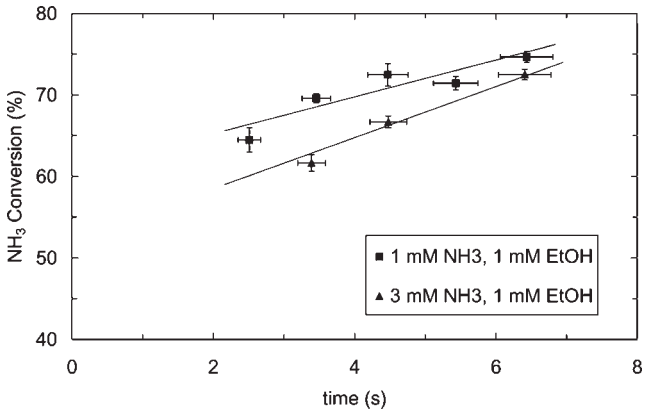

Figure 3. Ammonia conversion as a function of time for two different initial concentrations of ammonia.

$T = (701 \pm 4)^{\circ}C$, $P = 243 \pm 3$ bar, $[EtOH]_o = 0.97 \pm 0.02$ mM, and $\Phi = 1.00 \pm 0.05$.

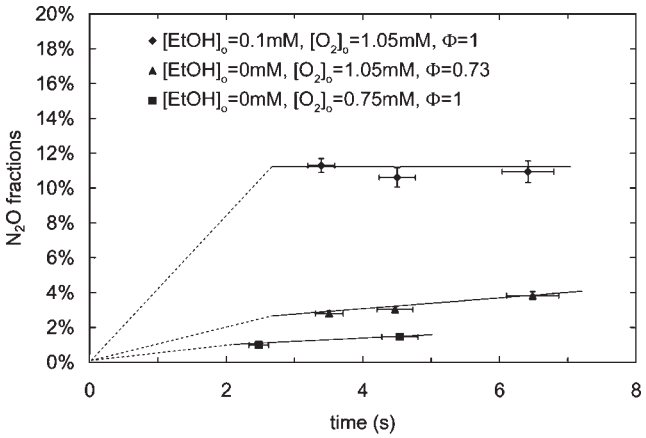

Figure 5. Nitrous oxide N fraction as a function of time for three different initial feed concentrations.

$T = (700 \pm 4)$°C and $P = 243 \pm 1$ bar.

version are quite dramatic for the addition of ethanol at equal initial molar concentrations as ammonia. Note that for initial ethanol concentrations of 0.5 and 1.0 mM the conversion at 6.5 s is not much greater than the conversion at 2.5 s; this indicates that the cooxidation enhancement is primarily occurring in the first 2 s of exposure to reaction conditions. Owing to comparable times required for achieving sufficient mixing of reactants and oxygen, we cannot unequivocally conclude that this is a purely kinetic effect. To underscore the effect that ethanol has on the rate of ammonia oxidation, at $T = (699 \pm 5)^{\circ}C$, $P = 243 \pm 3$ bar, $[NH_3]_o = 1.00 \pm 0.08$ mM, $\Phi = 0.95 \pm 0.05$, and $\tau = 2.5 \pm 0.2$ s, the addition of 0.5 mM ethanol results in a $(164 \pm 25)\%$ increase in ammonia conversion and the addition of 1.0 mM ethanol results in a $(224 \pm 29)\%$ increase.

Initial ammonia concentration has a much smaller effect on ammonia conversion, as illustrated in Figure 3. When the initial ammonia concentration is tripled with all other parameters held constant, the conversion decreases by less than 10%, which shows that ammonia has a small impact on the free-radical pool generated by ethanol.

Separating the effect of adding ethanol from the effect of adding oxygen for the stoichiometric oxidation of both ammonia and ethanol is complicated by the tendency towards reactor corrosion under conditions of excess oxygen and high temperatures. The only cooxidation experiments which could be repeated without ethanol at the same ammonia and oxygen concentrations were Runs 12–14, which corresponded to an initial ethanol concentration of 0.1 mM. Figure 4 compares the ammonia conversion data for three experiments at $T = 700^{\circ}C$ and $P = 246$ bar: $[NH_3]_o = 1$ mM and $[O_2]_o = 0.75$ mM ($\Phi = 1$), $[NH_3]_o = 1$ mM and $[O_2]_o = 1.05$ mM, ($\Phi = 0.73$), and $[NH_3]_o = [EtOH]_o = 1$ mM, $[O_2]_o = 1.05$ mM ($\Phi = 1$). The cooxidation enhancement of ethanol is approximately the same ($\sim$10%) as the enhancement gained when oxygen is added, which is consistent with what was seen for low concentrations of ethanol added to methylphosphonic acid (MPA).[25]

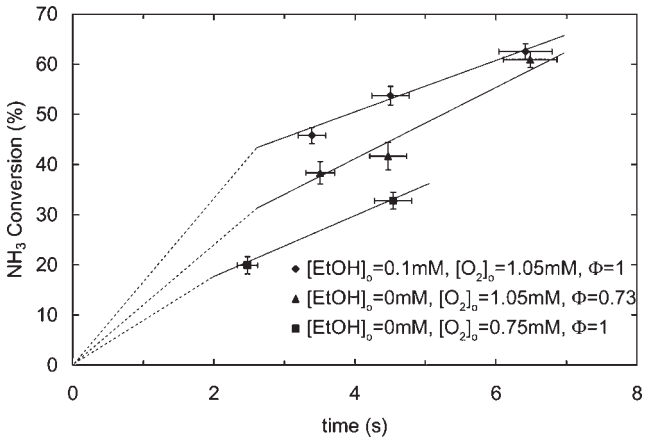

Figure 4. Ammonia conversion as a function of time for three different initial feed concentrations.

$T = (700 \pm 4)$°C and $P = 243 \pm 1$ bar.

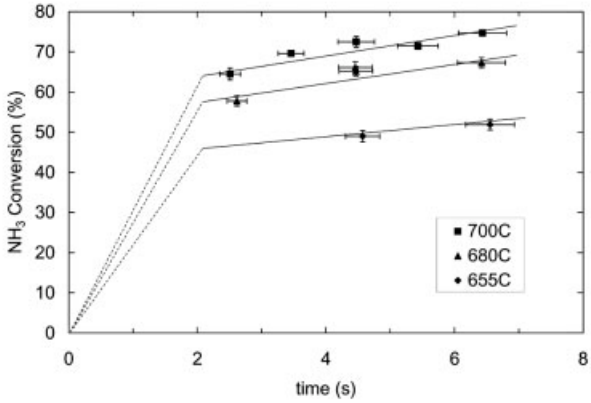

Figure 6. Ammonia conversion as a function of time for three different temperatures.

$P = 243 \pm 3$ bar, $[NH_3]_o = 1.00 \pm 0.08$ mM, $[EtOH]_o = 0.97 \pm 0.04$ mM, and $\Phi = 0.97 \pm 0.03$.

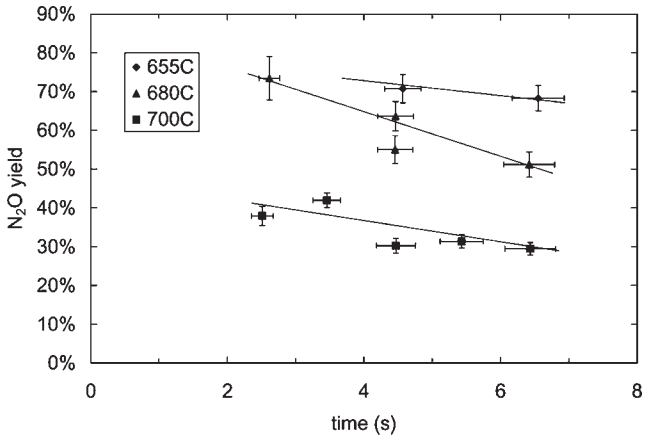

Figure 7. Nitrous oxide yield as a function of time for three different temperatures.

$P = 243 \pm 3$ bar, $[NH_3]_o = 1.00 \pm 0.08$ mM, $[EtOH]_o = 0.97 \pm 0.04$ mM, and $\Phi = 0.97 \pm 0.03$.

For the same three experiments, the effect of ethanol addition on product distribution is much more dramatic. Figure 5 shows the nitrous oxide fraction, defined as moles of nitrogen as N_2O in the effluent divided by moles of nitrogen as NH_3 in the feed, as a function of residence time for the same conditions as Figure 4. Adding oxygen has a small impact on N_2O formation, but the addition of ethanol causes the N_2O fraction to more than triple. The N_2O fraction remains constant over time for the ethanol co-oxidation data, which corroborates our theory that most of the cooxidation enhancement is happening in the first 2 s of residence time. From 3.5 to 6.5 s, ammonia continues to oxidize, but it predominantly oxidizes to N_2. Over time, this causes the N_2O yield, defined as moles of nitrogen as N_2O in the effluent divided by moles of nitrogen as NH_3 consumed in the reactor, to decrease as N_2O is diluted by additional N_2.

The effect of temperature on both ammonia conversion and N_2O yield was explored at $P = 246$ bar, $[NH_3]_o = [EtOH]_o = 1$ mM, and $\Phi = 1$. Figure 6 shows that conversion ranges from 50% at $T = 655$°C to 65–75% at $T = 700$°C, and at all three temperatures most of the cooxidation enhancement occurs in the first 2 s. Figure 7 shows that for equimolar mixtures of ammonia and ethanol, very high N_2O yields are possible, up to 73% at $T = 680$°C. As temperature increases, N_2O yield decreases to 30–40% at $T = 700$°C. Previous studies have shown that matching product distributions is the most reliable method for validating elementary reaction rate mechanisms,[26] so the N_2O yield data will be key to the development of an ammonia–ethanol cooxidation model.

Conclusions

Cooxidation of ammonia with ethanol in SCW indicates that ethanol had a dramatic effect on both the rate of ammonia oxidation and the product distribution. For example, at a 2.5 s residence time and stoichiometric oxygen conditions, ammonia conversion increased from 20 to 65% when a molar equivalent of ethanol was added to the organic feed at $T = 700$°C, $P = 246$ bar, and $[NH_3]_o = 1$ mM. Nitrous oxide yields for cooxidation experiments ranged from 40% at $T = 700$°C to over 70% at $T = 655$ and 680°C, compared to yields between 4 and 13% for pure ammonia oxidation under similar conditions. The cooxidation enhancement primarily occurred during the first 2 s of residence time, after which ammonia destruction proceeded more slowly and predominantly to form N_2. The rapid reaction rate underscores the need for data taken at shorter residence times than are possible for our current reactor system. The experimental observations in this study will be used to guide the development of an elementary reaction rate mechanism for the cooxidation of ammonia and ethanol in SCW in an upcoming article.

Acknowledgments

The authors acknowledge support provided by the Army Research Office (Award No. W911NF-05-1-0522), Shell Oil, Malaysian University of Science and Technology, and the Martin Family Society of Fellows for Sustainability. The authors also thank Professors Bill Green, Ken Smith, K.C. Swallow, and Bernhardt Trout and other members of the MIT Supercritical Fluids research group for their advice and suggestions during the course of the study. Stephanie Lee and Adam Madlinger were especially helpful in providing experimental assistance when needed.

Literature Cited

1. Modell M. Supercritical water oxidation. In: Freeman HM, editor. *Standard Handbook of Hazardous Waste Treatment and Disposal*. New York: McGraw Hill, 1989:8.153–158.168.
2. Tester JW, Holgate HR, Armellini FJ, Webley PA, Killilea WR, Hong GT, Barner HE. Supercritical water oxidation technology. In: Tedder WD, Pohland FG, editors. *Emerging Technologies in Hazardous Waste Management*, Vol. 518. Washington, DC: American Chemical Society, 1993:35–76.
3. Gloyna EF, Li L. Supercritical water oxidation research and development update. *Environ Progress*. 1995;14:182.
4. Savage PE, Gopalan S, Mizan TI, Martino CJ, Brock EE. Reactions at supercritical conditions: Applications and fundamentals. *AIChE J*. 1995;41:1723–1778.
5. Tester JW, Cline JA. Hydrolysis and oxidation in sub- and supercritical water: Connecting process engineering science to molecular interactions. *Corrosion*. 1999;55:1088.
6. Savage PE. Organic chemical reactions in supercritical water. *Chem Rev*. 1999;99:603.
7. Shaw RW, Dahmen N. Destruction of toxic organic materials using supercritical water oxidation: Current state of the technology. In: Kiran E, editor. *Supercritical Fluids*. Netherlands: Kluwer Academic, 2000.
8. Kritzer P, Dinjus E. An assessment of supercritical water oxidation (SCWO)—Existing problems, possible solutions and new reactor concepts. *Chem Eng J*. 2001;83:207–214.
9. Holgate HR, Tester JW. Fundamental kinetics and mechanisms of hydrogen oxidation in supercritical water. *Combust Sci Technol*. 1993;88(5/6):369–397.
10. Holgate HR, Tester JW. Oxidation of hydrogen and carbon monoxide in sub- and supercritical water: Reaction kinetics, pathways, and water-density effects, Part 1: Experimental results. *J Phys Chem*. 1994;98:800–809.
11. Webley PA, Tester JW. Fundamental kinetics of methane oxidation in supercritical water. *Energy Fuels*. 1991;5:411–419.
12. DiNaro J, Tester J, Howard J, Swallow K. Experimental measurements of benzene oxidation in supercritical water. *AICHE J*. 2000; 46:2274–2284.
13. Sullivan PA, Tester JW. Methylphosphonic acid oxidation kinetics in supercritical water. *AIChE J*. 2004;50:673–683.
14. Schanzenbacher J, Taylor JD, Tester JW. Ethanol oxidation and hydrolysis rates in supercritical water. *J Supercrit Fluid*. 2002;22:139–147.
15. Taylor JD, Steinfeld JI, Tester JW. Experimental measurement of the rate of methyl *tert*-butyl ether hydrolysis in sub- and supercritical water. *Ind Eng Chem Res*. 2001;40:67–74.

16. Webley PA, Tester JW, Holgate HR. Oxidation kinetics of ammonia and ammonia-methanol mixtures in supercritical water in the temperature range 530–700°C at 246 bar. *Ind Eng Chem Res.* 1991; 30:1745–1754.
17. Ploeger JM, Madlinger AC, Tester JW. Revised global kinetic measurements of ammonia oxidation in supercritical water. *Ind Eng Chem Res.* 2006;45:6842–6845.
18. Segond N, Matsumura Y, Yamamoto K. Determination of ammonia oxidation rate in sub- and supercritical water. *Ind Eng Chem Res.* 2002;41:6020–6027.
19. Hong GT, Fowler PK, Killilea WR, Swallow KC. Supercritical water oxidation: Treatment of human waste and system configuration tradeoff study. Proceedings of 17th Intersociety Conference on Environmental Systems. July 13–15, 1987; Seattle, WA.
20. Cocero MJ, Alonso E, Torío R, Vallelado D, Fdz-Polanco F. Supercritical water oxidation in a pilot plant of nitrogenous compounds: 2-Propanol mixtures in the temperature range 500–750°C. *Ind Eng Chem Res.* 2000;39:3707–3716.
21. Ploeger JM, Green WH, Tester JW. Co-oxidation of methylphosphonic acid and ethanol in supercritical water: II. Elementary reaction rate model. *J Supercrit Fluids.* 2006;39:239–245.
22. DiNaro JL. Oxidation of benzene in supercritical water: experimental measurements and development of an elementary reaction mechanism. PhD Thesis. Cambridge, MA: Department of Chemical Engineering, Massachusetts Institute of Technology, 1999.
23. Phenix B, Dinaro J, Tester J, Howard J, Smith K. The effects of mixing and oxidant choice on laboratory-scale measurements of supercritical water oxidation kinetics. *Ind Eng Chem Res.* 2002;41: 624–631.
24. Dean JA. *Lange's Handbook of Chemistry*. New York: McGraw-Hill, 1992.
25. Ploeger JM, Bielenberg PA, Lachance RP, Tester JW. Co-oxidation of methylphosphonic acid and ethanol in supercritical water: I. Experimental results. *J Supercrit Fluids.* 2006;39:233–238.
26. Ploeger JM, Bielenberg PA, DiNaro Blanchard JL, Lachance RP, Taylor JD, Green WH, Tester JW. Modeling oxidation and hydrolysis reactions in supercritical water––Free radical elementary reaction networks and their applications. *Comb Sci Tech.* 2006;178(1–3): 363–398.

Manuscript received Oct. 21, 2006, and revision received Dec. 25, 2006.